Journal of Thermal Analysis and Calorimetry, Vol. 55 (1999) 511-530

APPLICATION OF STATISTICAL RATE THEORY OF INTERFACIAL TRANSPORT TO STUDY SOLID SURFACE HETEROGENEITY FROM CONTROLLED-RATE THERMAL DESORPTION

F. Villiéras[1*], *L. J. Michot*[1], *G. Gérard*[1], *J. M. Cases*[1] *and W. Rudzinski*[2**]

[1]Laboratoire Environnement et Minéralurgie, INPL et UMR 7569 du CNRS, Ecole Nationale Supérieure de Géologie, BP 40, 54 500 Vandoeuvre les Nancy, France
[2]Department of Theoretical Chemistry, Faculty of Chemistry, Maria Curie-Skłodowska University, Pl. Marii Curie-Skłodowskiej 3, Lublin 20-031, Poland

Abstract

Controlled-rate thermodesorption (CRTD) spectra are obtained by adjusting the heating rate in such a way that the rate of desorption can be constant. A quantitative analysis of the obtained spectra is presented, based on application of the statistical rate theory of interfacial transport (SRTIT) to describe both adsorption and desorption kinetics. The SRTIT approach relates the rates of adsorption and desorption to the chemical potentials of the adsorbate in the gaseous and in the adsorbed phases. This quantitative analysis of the CRTD spectra yields the condensation approximation for the actual adsorption energy distribution. For the purpose of illustration, an analysis is made of water desorption from a synthetic apatite mineral under CRTD and classical TPD conditions. The influence of the adsorption and desorption rates is also discussed.

Keywords: apatite, CRTD spectra, surface heterogeneity, thermal desorption

Introduction

The commonly used quantitative measure of the energetic heterogeneity of a solid surface is the differential distribution of the number of adsorption sites among the corresponding values of adsorption energy ε, $\chi(\varepsilon)$, normalized to unity:

$$\int_{\Omega_\varepsilon} \chi(\varepsilon)d\varepsilon = 1 \qquad (1)$$

* Author for correspondence: Fax: (33)383 575 403 E-mail: fvillier@ensg.u-nancy.fr
**Fax: (48)81 537 5685 E-mail: rudzinsk@hermes.umcs.lublin.pl

1418–2874/99/ $ 5.00

Akadémiai Kiadó, Budapest
Kluwer Academic Publishers, Dordrecht

where Ω_ε is the physical domain of ε on the investigated solid surface. The experimentally observed total fractional coverage of the solid surface, $\theta_t(p,T)$, is then given by the following average:

$$\theta_t(p,T) = \int_{\Omega_\varepsilon} \theta(\varepsilon,p,T)\chi(\varepsilon)d\varepsilon \qquad (2)$$

where $\theta(\varepsilon,p,T)$ is a theoretical expression describing the fractional coverage of sites having adsorption energy within the interval $(\varepsilon,\varepsilon+d\varepsilon)$. This expression is usually called the 'local adsorption isotherm', whereas the function $\chi(\varepsilon)$ is the 'adsorption energy distribution'.

Various expressions have been accepted to represent the local adsorption isotherm, depending on the physicochemical nature of the adsorbate-solid interface. Equations (2) is frequently treated as an integral equation for the unknown function $\chi(\varepsilon)$, because $\theta(\varepsilon,p,T)$ is known from theory, whereas $\theta_t(p,T)$ is found from experiment. A variety of methods have been used to solve this integral equation; a description can be found in two recently published monographs [1, 2].

Static (equilibrium) measurements of the adsorption isotherms $\theta_t(p,T)$, however, apply mostly to physisorption systems where the solid-adsorbate bonds are relatively weak. The equilibrium isotherms can measured at either low or room temperatures.

Studies of equilibrium isotherms of chemisorption would require the application of high-temperature regimes, which involves well-known technical problems. Accordingly for studies of the surface energetic heterogeneity in chemisorption systems, another technique has commonly been applied: temperature-programmed desorption (TPD). Amenomiya and Cvetanovic published the principles of this method in 1963 [3], and 6 years later, their theoretical paper was published on the application of such experiments to study surface heterogeneity [4, 5]. In fact, the TPD technique has primarily been used to study the surface energetic heterogeneity of catalysts and adsorbents. The various peaks observed in TPD diagrams have been ascribed to various kinds of surface adsorption sites, characterized by different activation energies for desorption [6–9].

In TPD, the sample is heated at a constant rate. As a consequence, thermal desorption proceeds at different speeds (different pressures) at different temperatures. The calculation of the adsorption energy distribution function involves a consideration of the simultaneous variation in P and T. This can be overcome by carring out desorption at constant speed (pressure), using 'constant-rate thermal analysis' (CRTA), also called reciprocal evolved-gas-detection thermal analysis, described by Rouquerol in 1970 [10–12]. The high sensitivity of CRTA allows controlled-rate thermal desorption (CRTD) to be carried out on samples with specific surface areas higher than 1 $m^2\ g^{-1}$. One then obtains a desorption isobar curve. A very similar type of experiment, based on constant mass loss, was proposed independently by the Pauliks in Budapest at the beginning of the 1960s [13–15].

In the case of TPD, great progress has recently been made towards a quantitative interpretation of desorption spectra with respect to surface energetic heterogeneity [6–12]. In contrast, CRTD spectra have rather been interpreted on a qualitative level. The purpose of the present paper is to propose a first quantitative interpretation of CRTD spectra, based on application of the statistical rate theory of interfacial transport.

Theoretical principles

In the theory of TPD, the absolute rate theory (ART) approach is still most frequently used [16]. According to ART, the change in the surface coverage θ with time, t is given by

$$\frac{\partial\theta}{\partial t} = K_a p(1-\theta)^s \exp\left\{\frac{-\varepsilon_a}{kT}\right\} - K_d\theta^s \exp\left\{\frac{-\varepsilon_d}{kT}\right\} \tag{3}$$

where s is the number of sites involved in an elementary adsorption-desorption process, p is the pressure in the gas phase, ε_a and ε_d are the activation energies for adsorption and desorption, respectively, and K_a and K_d are slightly temperature-dependent constants. Further, T and k are the absolute temperature and the Boltzmann constant, respectively.

The first term on the r.h.s. of Eq. (3) represents the rate of adsorption, and the second term represents the rate of desorption. Let us consider for simplicity the case when s=1. Then, at equilibrium when $\partial\theta/\partial t$=0, Eq. (3) yields the Langmuir isotherm equation:

$$\theta^{(e)}(\varepsilon,p,T) = \frac{K_p \exp\left\{\frac{\varepsilon}{kT}\right\}}{1 + K_p \exp\left\{\frac{\varepsilon}{kT}\right\}} \tag{4}$$

where K=K_a/K_d and ε=(ε_d–ε_a), while the superscript (e) refers to equilibrium conditions. Usually, TPD experiments are carried out under conditions where the (first) readsorption term on the r.h.s. of Eq. (3) can be neglected. Hence:

$$\frac{\partial\theta}{\partial t} = -K_d\theta \exp\left\{\frac{-\varepsilon_d}{kT}\right\} \tag{5}$$

However, the inability of Eq. (5) to represent thermodesorption in real adsorption systems was reported long ago, and was ascribed to surface energetic heterogeneity, to interactions between adsorbed molecules, or to both of these factors. In chemisorption systems, the gas-solid interactions are usually much stronger than the gas-gas interactions, and the surface energetic heterogeneity is therefore commonly assumed to be the dominant factor.

The elucidation of quantitative information concerning surface heterogeneity from TPD spectra usually starts from the assumption that the adsorption proceeds in an ideally stepwise fashion, in the sequence of increasing activation energies for desorption. This means that, at any surface coverage θ_t, the kinetics of desorption should be described by the equation

$$\frac{\partial\theta_t}{\partial t} = -K_d\theta_t \exp\left\{\frac{-\varepsilon_d(\theta_t)}{kT}\right\} \tag{6}$$

To elucidate the function $\varepsilon_d(\theta_t)$, the method of variable heating rate is most frequently applied, and the obtained spectra are next studied in terms of the following Arrhenius plot:

$$\ln\frac{-\partial\theta_t/\partial_t}{\theta_t} = \ln K_d - \frac{\varepsilon_d}{kT} \tag{7}$$

Then, however, when this method is applied to experimental TPD spectra, it appears that not only ε_d varied with surface coverage. Surprisingly, K_d also varies over several orders of magnitude as a rule. This can best be seen in the excellent review by Zhdanov [17], where $\varepsilon_d(\theta_t)$ and $K_d(\theta_t)$ functions are collected for a variety of adsorption systems.

Seebauer *et al.* [18] have reviewed different theoretical representations for the preexponential factor K_d. None of them was able to account for such strong variations in K_d with θ_t. Thus, as early as at the beginning of the 1950s, Kisliuk [19] launched his idea of the 'precursor state'. Twenty years later, King [20] developed this idea further by assuming that two precursor states may exist, one over the filled sites, and the second one over empty sites. A year later, Gorte and Schmidt [21] proposed yet another concept of the precursor states. A brief description of the 'precursor state approaches' can be found in the review by Lombardo and Bell [9]. These approaches have mainly been used to study the desorption kinetics in systems with well-defined (nearly homogeneous) solid surfaces. The studies of surface energetic heterogeneity were still based on the traditional ART approach.

At the beginning of the 1980s, a new family of approaches to adsorption/desorption kinetics appeared. A common fundamental feature of these approaches is that they relate the adsorption/desorption rate kinetics to the chemical potential of the adsorbed molecules. The approach proposed by Nagai [22, 23] in 1985 should, for historical reasons, be considered first. This is because some idea of the approach can be traced in the works by de Boer [24]. In this approach, the rate of desorption R_d is represented by

$$R_d = \nu\exp\left(\frac{\mu^s - E_d}{kT}\right) \tag{8}$$

where ν is a pre-exponential factor, μ^s is the chemical potential of the adsorbed molecules and E_d is the energy for desorption. Nagai's approach, like two others which will be discussed shortly, is especially useful for describing adsorption/desorption processes that are not far from equilibrium. The fundamental assumption here is that, at 'quasi-equilibrium', the transient states of the adsorbed phase are close to the equilibrium ones corresponding to the same surface coverage. In terms of statistical thermodynamics, this means that all the correlation functions are the same.

In Eq. (8), E_d has the same meaning of the difference between the potential energies in the adsorbed and activated states. As a matter of fact, Nagai's approach was aimed at improving ART by taking into account the entropic effects. The appearance of Nagai's approach immediately gave rise to strong debate [25–27]. Recently, however, Nagai [28] has presented an impressive example: the adsorption system described by the hard hexagon model, where his Eq. (8) appears to be superior in describing the corresponding TPD spectra.

The second theoretical approach that belongs in the new family of approaches, referring to the chemical potential of adsorbed molecules, was developed by Kreuzer and coworkers [30–33] in 1988. Their expression for the rate of desorption R_d has the following form:

$$R_d = S(\theta)\alpha_s kT(2\pi mkT/h^3)q_o^g \exp\left(\frac{\mu^s}{kT}\right) \tag{9}$$

where α_s is the area of adsorption sites, q_g^o is the gas molecule partition function corresponding to the internal degrees of freedom, m is the mass of the molecule, h is Planck's constant and $S(\theta)$ is a 'sticking coefficient'. This coefficient cannot be obtained from thermodynamic arguments, but must be calculated in some way from microscopic theory, or be postulated in a phenomenological approach, based on experimental evidence for a particular system or some simple arguments.

Assuming that the transport between two phases at thermal equilibrium primarily results from single molecular events, Ward and coworkers developed the following equation for the rate of transport between a gas and a solid phase [33, 35], using a first-order perturbational analysis of the Schrodinger equation, and the Boltzmann definition of entropy:

$$\frac{\partial\theta}{\partial t} = K'_{gs}\left[\exp\left\{\frac{\mu^g - \mu^s}{kT}\right\} - \exp\left\{\frac{\mu^s - \mu^g}{kT}\right\}\right] \tag{10}$$

where μ^g and μ^s are the chemical potentials of the molecule in the gas phase and in the adsorbed phase, respectively, and K'_{gs} is a constant.

Let μ^g be the chemical potential of an ideal gas, and μ^s be the expression corresponding to the Langmuir model of adsorption (one-site-occupancy monolayer adsorption, with no interactions between the adsorbed molecules):

$$\mu^g = \mu_o^g + kT\ln p, \text{ and } \mu^s = kT\ln \frac{\theta}{q^s(1-\theta)} \tag{11}$$

where q^s is the molecular partition function of the adsorbed molecules. Equation (10) then takes the following form:

$$\frac{\partial\theta}{\partial t} = 2K'_{gs} \sinh\left\{\frac{\mu_o^g}{kT} + \ln\left(\frac{q^s p(1-\theta)}{\theta}\right)\right\} \tag{12}$$

The energetic heterogeneity of actual solid surfaces is demonstrated mainly as the variation in the adsorption energy ε in the molecular partition function $q^s = q_o^s \exp\{(q_1^s+\varepsilon)/kT\}$, where q_1^s is a given constant for all adsorption sites. It may, for instance, comprise the value coming from the low-temperature limit of vibrational partition functions. With this notation, Eq. (12) takes the form

$$\frac{\partial\theta}{\partial t} = 2K'_{gs} \sinh\left\{\frac{\varepsilon + q_1^s + \mu_o^g}{kT} + \ln\left(q_o^s p\frac{1-\theta}{\theta}\right)\right\} \tag{13}$$

From a theoretical point of view, experiments carried under non-equilibrium and quasi-equilibrium conditions must be described by Eq. (13) with the same set of constants. This will be tested by using the CRTA device in the case of water desorption from apatite.

Materials and methods

Constant-rate thermal analysis (CRTA)

In this method, the heating rate is controlled by the sample, and depends on the rate of desorption of adsorbed species. The rate of gas desorption is maintained constant (or controlled) by adjusting the temperature over the entire temperature range of the experiment. The rate of desorption, or gas flow, is maintained by keeping constant (at a chosen value) the pressure drop through a restriction leading to the pump (Fig. 1). The application of pressure measurement to control the rate of desorption through adjustment of the heating rate yields a significant enhancement of the resolution.

When desorption occurs, molecules leave the surface. This leads to a pressure increase over the sample. In order to keep the pressure constant, the heating is stopped, and the system remains at constant temperature until the desorption starts to decrease. The temperature is then increased again until another significant desorption process begins. For a constant rate of vapour loss, the temperature *vs.* time data may be converted immediately into temperature *vs.* mass loss data, if the total mass loss is measured at the end of the experiment. If different gases are evolved from the surface, a mass spectrometer placed just above the restriction allows determination of their partial pressures.

Rouquerol and coworkers [10–12] have extensively discussed the multiple advantages of this method: the technique allows the detection of the desorption of very small quantities; the determination of equilibrium temperature is more accurate than in conventional thermal analysis; and temperature and pressure gradients within the sample can be eliminated if the desorption rate is low enough. Furthermore, if needed, the experiments can be carried out directly with the sample cell used for gas adsorption experiments.

One great advantage of CRTD is that it can be operated under both non-equilibrium and quasi-equilibrium conditions, using the same device. Accordingly, one can study both kinetics of desorption and adsorption equilibria. However, although the principles of CRTD were described as long ago as in 1970, the recorded experimental desorption data were mostly interpreted on a qualitative level, and no attempts have been made to recover the adsorption energy distribution. For instance, CRTA has been applied to study the amount of water adsorbed in microporous clay minerals, such as sepiolite and palygorskite [36, 37], the features of exchangeable cations of homoionic montmorillonites [38, 39], and the different molecules naturally adsorbed on the surface of talc [40]. Recently, CRTA has also been used to study the desorption of preadsorbed chemicals such as phenol from activated carbons [41, 42].

Sample

The sample used to test the applicability of CRTA for studies of surface energetic heterogeneity was a pure and synthetic hydroxyapatite provided by Stauffer as 'tricalcium phosphate quality food'. It is a calcium phosphate, $Ca_{10}(PO_4)_6(OH)_2$. The sample was first micronized under gaseous conditions in order to separate the microcrystals from the aggregates.

After outgassing at 270°C, its BET nitrogen specific surface area was 85 $m^2\ g^{-1}$, and the monolayer water vapour adsorption capacity was 1.07 mmol g^{-1}.

Results and discussion

Thermal analysis

Three thermal desorption experiments were performed with the same sample. 0.4 g of apatite was outgassed under CRTA conditions up to 575 K under 2 Pa. The sample was then kept at 575 K during 6 h. Water vapour adsorption was carried out at 303 K, using an outgassed vapour source maintained at 297 K. The adsorption relative pressure was then roughly 0.7. The system was next outgassed at 297 K up to the experimental set pressure point. Mass loss was recorded in order to determine the amount of water still adsorbed on the surface. CRTA was recorded up to 575 K.

The recorded CRTD spectra are presented in Fig. 2, and the related experimental conditions are described in Table 1. Experiments 1 and 2 were performed

under CRTA conditions. The temperature variation was independent of time. Experiment 3 was performed under TPD-like conditions, as the pressure of the adsorbed species never reached the set pressure. In this case, the temperature increased roughly linearly with time, at a heating rate of about 5 K min^{-1}. However, the time dependence of the temperature shows that regulation was not perfect during the experiment, as a small plateau can be observed at around 470 K.

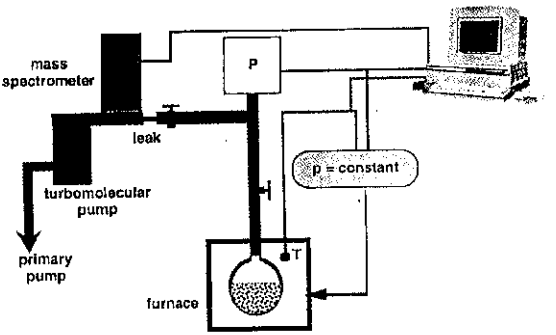

Fig. 1 Schematic representation of CRTA set-up

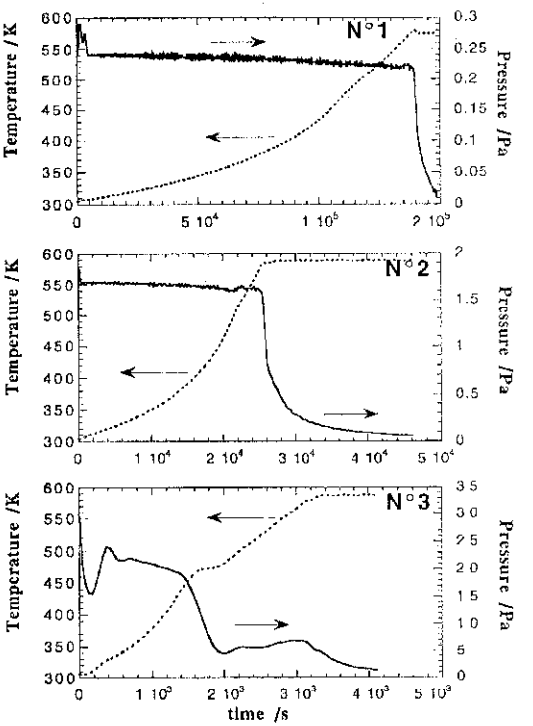

Fig. 2 Pressure and temperature evolution as a function of time for experiments 1, 2 and 3

Table 1 Experimental conditions under which thermodesorption experiments were carried out

Experiment	Set pressure/ Pa	Heating rate/ $^{\circ}C\ min^{-1}$	Initial surface coverage/θ_i
1	0.23	adjusted	0.56
2	1.67	adjusted	0.71
3		5	1.125

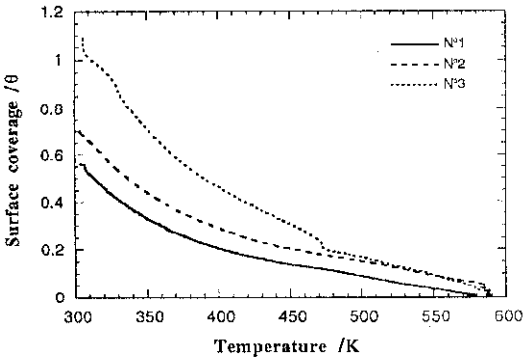

Fig. 3 Evolution of surface coverage with temperature in experiments 1, 2 and 3

For experiments 1 and 2, the surface coverage evolution *vs.* temperature was calculated by integration of the signal m/z=18 from the mass spectrometer. In experiment 3, this evolution was calculated by integration of the pressure evolution, as preceding calibrations showed that the flow rate of water output is directly proportional to the pressure measured over the sample. Curve were normalized to the initial surface coverage (Table 1). The evolution of surface coverage *vs.* temperature (Fig. 3) displays similar features in experiments 1 and 2. As could be expected, the evolution observed in experiment 3 is considerably different.

Adsorption energy distribution and quasi-equilibrium assumption

If the desorption rate is small enough (quasi-equilibrium), the adsorption rate and desorption rate become equal. The adsorption equation derived from Eq. (13) then takes the Langmuir form:

$$\theta = \frac{q_o^s p \exp\left(\frac{\varepsilon + \Delta}{kT}\right)}{1 + q_o^s p \exp\left(\frac{\varepsilon + \Delta}{kT}\right)} \qquad (14)$$

where $\Delta=\mu_o^g+q_i^s$. Equation (14) can be rewritten in a Fermi-like form:

$$\theta = \frac{\exp\left\{\frac{\varepsilon - \varepsilon_c}{kT}\right\}}{1 + \exp\left\{\frac{\varepsilon - \varepsilon_c}{kT}\right\}} \tag{15}$$

where

$$\varepsilon_c = \Delta - kT\ln(q_o^s p) \tag{16}$$

For the limit $T \to 0$, the function $\theta(\varepsilon)$ in Eq. (15) becomes the following step function, $\theta_c(\varepsilon)$:

$$\lim_{T \to 0} \theta(\varepsilon) = \theta_c(\varepsilon) = \begin{cases} 0, \text{ for } \varepsilon < \varepsilon_c \\ 1, \text{ for } \varepsilon > \varepsilon_c \end{cases} \tag{17}$$

At finite, but not too high temperatures, $\theta(\varepsilon)$ will resemble the step function (Fig. 4). In the case of adsorption on a heterogeneous surface, for the limit $T \to 0$, the desorption will proceed in an ideally stepwise fashion, i.e. the desorption will proceed gradually in the sequence of increasing adsorption energies. The sites whose energies are smaller than ε_c will remain uncovered (Fig. 4). Thus:

$$\theta_t(\varepsilon_c) = \int_{\varepsilon_c}^{\infty} \chi(\varepsilon) d\varepsilon \tag{18}$$

The energy distribution problem is similar to that considered in the papers on adsorption equilibria on heterogeneous solid surfaces. There, a variety of methods have been used to elucidate the adsorption energy distribution from measured adsorption data [1, 2]. Probably the most fruitful ones were based on improving the solution for $\chi(\varepsilon)$, obtained by using the condensation approximation (CA) for $\chi(\varepsilon)$, usually denoted $\chi_c(\varepsilon_c)$:

$$\chi_c(\varepsilon_c) = -\frac{\partial \theta_t}{\partial \varepsilon_c} = -\int_0^{\infty} \left(\frac{\partial \theta}{\partial \varepsilon_c}\right) \chi(\varepsilon) d\varepsilon \tag{19}$$

The comparison of experiments performed at different pressures allows the consideration of q_o^s as a best-fit parameter which must be chosen in order to obtain superposition of the experimental curves:

$$\chi_c(\varepsilon_c) = -\frac{\partial \theta_t}{\partial \varepsilon_c} \tag{20}$$

Condensation energy distributions calculated by accepting various values of q_o^s are presented in Fig. 5. The quasi-equilibrium conditions could be considered

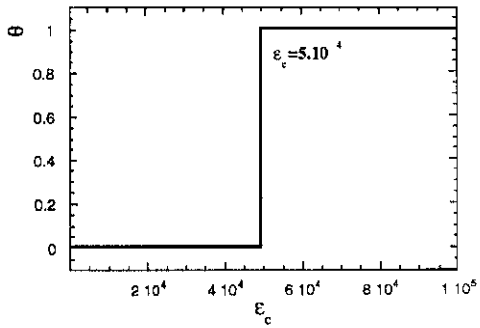

Fig. 4 Example of step function for $\varepsilon_c=5\times10^4$

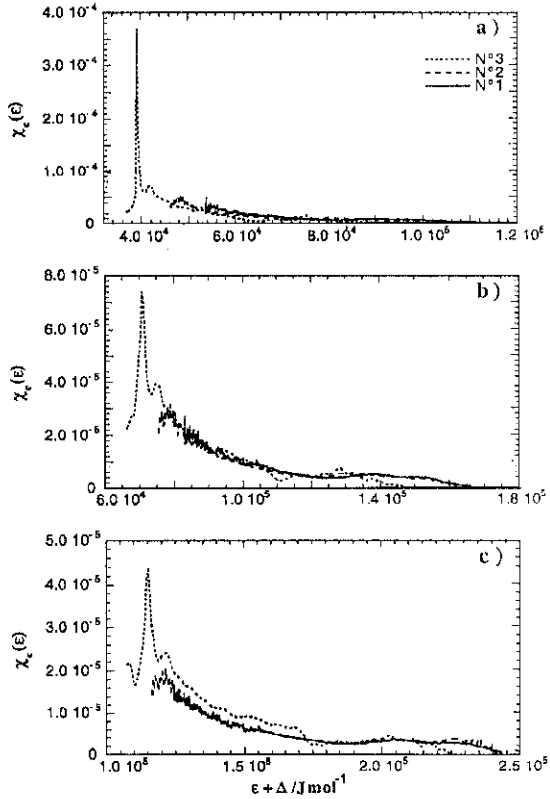

Fig. 5 Energy distribution function $\chi_c(\varepsilon)$ calculated from Eq. (20), when ε_c is defined as in Eq. (16) for q_o^s=a) 10^{-8} Pa^{-1}, b) 10^{-13} Pa^{-1} and c) 10^{-20} Pa^{-1}

as nearly fulfilled in experiments 1 and 2, as the calculated mean desorption rates were 3.1×10^{-6} θ/s and 2.7×10^5 θ/s, respectively. As mentioned above, quasi-equilibrium was not achieved in experiment 3. The test of the influence of q_o^s on the

obtained distribution shows that a relatively good superposition of the distributions derived from experiments 1 and 2 can be obtained for q_o^s ranging between 10^{-10} and 10^{-20}. As shown in Fig. 5, the value of q_o^s dramatically influences the energy scale, which is shifted towards higher energy when q_o^s decreases. The best result was obtained for $q_o^s=10^{-13}$, but its theoretical verification is almost impossible. This is one of the most difficult problems in adsorption science. The energy distributions calculated from experiment 3 never match the two others. Of course, such a result is to be expected, due to the non-equilibrium conditions required for the present approach. Furthermore, the assumption of equilibrium for this experiment should be reflected by an overestimation of the energy scale with regard to the two other experiments. This is obtained with q_o^s values lower than 10^{-15}.

Thus, kinetic effects are to be taken into account, as it will be shown in the following sections.

Non-equilibrium conditions

Two situations are encountered in our experiments, depending on the way in which thermodesorption is carried out. In the case of TPD, the rate of readsorption can be neglected, as the heating rate favours desorption. In CRTD, the rates of both readsorption and desorption have to be taken into account.

Adsorption energy distribution without readsorption rate

When the readsorption rate is negligible as compared to the desorption rate, Eq. (13) becomes

$$\frac{\partial\theta}{\partial t} = -K'_{gs}\,\frac{1}{q_o^s p}\,\frac{\theta}{1-\theta}\exp\left\{-\frac{\varepsilon+\Delta}{kT}\right\} \tag{21}$$

The adsorption isotherm equation derived from the above expression is

$$\theta = \frac{\dfrac{q_o^s p}{K'_{gs}}\left(-\dfrac{\partial\theta}{\partial t}\right)\exp\left\{\dfrac{\varepsilon+\Delta}{kT}\right\}}{1+\dfrac{q_o^s p}{K'_{gs}}\left(-\dfrac{\partial\theta}{\partial t}\right)\exp\left\{\dfrac{\varepsilon+\Delta}{kT}\right\}} \tag{22}$$

which can be written in the same form as Eq. (15), with ε_c defined as follows:

$$\varepsilon_c = -\Delta - kT\ln\left[\frac{q_o^s p}{K'_{gs}}\left(-\frac{\partial\theta}{kT}\right)\right] \tag{23}$$

According to the CA approach (accuracy level) accepted here, desorption proceeds in an ideally stepwise fashion in a sequence of decreasing adsorption energies. The 'desorption front' is located on the sites with adsorption energy equal to ε_c. This means that the kinetics of desorption is proportional to the 'local' rate of desorption from these sites, and to the population of these sites, $\chi_c(\varepsilon_c)$. Thus, the rate of desorption is to be expressed as follows:

$$\frac{\partial\theta_t}{\partial t} = \chi_c(\varepsilon_c)\left(\frac{\partial\theta(\varepsilon)}{\partial t}\right)_{\varepsilon=\varepsilon_c} \tag{24}$$

Then:

$$\frac{\partial\theta_t}{\partial t} = -\chi_c(\varepsilon_c)\frac{K'_{gs}}{q^s_o p}\exp\left\{-\frac{\varepsilon_c+\Delta}{kT}\right\} \tag{25}$$

From a consideration of Eq. (20), one can write

$$\chi_d(\varepsilon_c) = -\frac{\partial\theta_t}{\partial\varepsilon_c} = -\frac{\partial\theta_t}{\partial t}\left(\frac{\partial\varepsilon_c}{\partial t}\right)^{-1} \tag{26}$$

The combination of Eqs (25) and (26) gives

$$\frac{\partial\varepsilon_c}{\partial t} = \frac{K'_{gs}}{q^s_o p}\exp\left\{-\frac{\varepsilon_c+\Delta}{kT}\right\} \tag{27}$$

The relationship between ε_c, t and T can be obtained by solving the differential equation (27) throughout the experiment.

In our calculations, the ratio $q=q^s_o/K'_{gs}$ was regarded as a single constant. The main difficulty was to choose the initial value of ε_c. In consequence of the kinetic conditions assumed here, the starting energy should be lower than that derived from the equilibrium conditions. Thus, $\varepsilon_c(t=0)$ was first estimated from the equation for equilibrium, Eq. (16), and was next lowered, until an acceptable shape was obtained. For experiment 3, $\varepsilon_c(t=0)$ was chosen in order to conserve the low-energy minimum observed for the equilibrium conditions. For the two other experiments, a corrected value was chosen in order to superimpose, if possible, this first point on the condensation energy distribution curve of experiment 3. The differential equation was next solved by using an iterative procedure, until the maximum relative error was less than 0.1% for each calculated point. Energy distributions were then calculated from Eq. (26). The results obtained are presented in Fig. 6 for $q=10^{-20}$ and 10^{-23}. The numerical integration procedure applied to solve Eq. (27) has the result that the distributions calculated from experiments 1 and 2 are less noisy than those derived from the equilibrium assumption. The tests show that it is impossible to obtain relevant results for q greater than 10^{-13}.

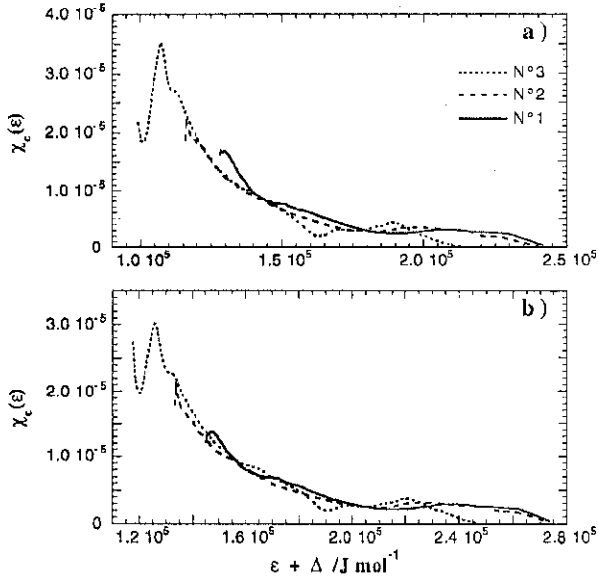

Fig. 6 Energy distribution function $\chi_c(\varepsilon)$ calculated from Eqs (26) and (27), when q=a) 10^{-20} Pa^{-1} and b) 10^{-23} Pa^{-1}

The energy scales are shifted toward higher energies when q decreases, as already observed for equilibrium conditions.

A relatively good superposition of the calculated distributions can be obtained for $q=10^{-20}$. For instance, in experiments 2 and 3 good superposition is observed in the low-energy range of experiment 2. However, it was impossible to attain superposition in the low-energy region of experiment 1 with experiments 2 and 3. Furthermore, $\varepsilon_c(t=0)$ had to be increased, which is physically unjustified, in order to arrive at the shape observed in experiment 3. In the region of high energies, acceptable superposition was achieved for experiments 1 and 2. For $q=10^{-23}$, superposition of the distribution curves was less good. However, it can be observed that the distribution computed from experiment 3 ranges between those obtained for experiments 1 and 2 in their low-energy region. As for $q=10^{-20}$, it is also observed that it is not possible to match the beginning of experiment 1 with experiment 3. These phenomena can be ascribed to the fact that the readsorption rate cannot be neglected in experiment 1, because of the very low desorption rate. The influence of the readsorption rate is taken into account in the extended treatment presented in the next section.

Adsorption energy distribution with readsorption rates

When the rate of desorption is low, the readsorption rate can not be considered negligible. Equation (13) must then be solved.

On using the hyperbolic sine expansion series, Eq. (13), one can write

$$\frac{\partial\theta}{\partial t} = 2K'_{gs}\left\{\left[\frac{\varepsilon+\Delta}{kT} + \ln\left(q_o^s\frac{1-\theta}{\theta}\right)\right] + \frac{1}{3!}\left[\frac{\varepsilon+\Delta}{kT} + \ln\left(q_o^s p\frac{1-\theta}{\theta}\right)\right]^3 + \ldots \right.$$
$$\left. + \frac{1}{(2n+1)!}\left[\frac{\varepsilon+\Delta}{kT} + \ln\left(q_o^s p\frac{1-\theta}{\theta}\right)\right]^{2n+1} + \ldots\right\} \quad (28)$$

If the experimental conditions are such that the system is close to equilibrium, the expression

$$E = \frac{\varepsilon+\Delta}{kT} + \ln\left(q_o^s\, p\,\frac{1-\theta}{\theta}\right) \quad (29)$$

should be close to zero. The terms of order greater than 3 in the series can then be neglected, and an equation for the surface coverage θ can be derived from Eq. (29):

$$\theta = \frac{q_o^s\, p\, \exp\left\{\dfrac{\varepsilon+\Delta}{kT} - \dfrac{2\partial\theta/\partial t}{K'_{gs}}\right\}}{1 + q_o^s\, p\, \exp\left\{\dfrac{\varepsilon+\Delta}{kT} - \dfrac{2\partial\theta/\partial t}{K'_{gs}}\right\}} \quad (30)$$

Equation (30) can be written in the same form as Eq. (15) by defining ε_c as follows:

$$\varepsilon_c = -\Delta + 2kT\frac{\partial\theta/\partial t}{K'_{gs}} - kT\ln(q_o^s\, p) \quad (31)$$

As in the previous section, a differential equation similar to Eq. (27) is obtained:

$$\frac{\partial\varepsilon_c}{\partial t} = -2K'_{gs}\ \sinh\left\{\frac{\varepsilon_c+\Delta}{kT} + \ln(q_o^s p)\right\} \quad (32)$$

Calculations have been performed in the same way as for desorption-controlled kinetics. In the present case, the determination of the condensation energy distributions depends on two parameters, q_o^s and K'_{gs}. First, the role played by these two parameters was studied, and typical results are presented in Fig. 7.

Equation (32) suggests that K'_{gs} and E (defined in Eq. (29)) have reverse effects as, for a given total desorption rate, their product should be constant. Then, for high values of K'_{gs}, E will be close to zero, meaning that the actual condensation energy is close to the equilibrium condensation energy, defined in Eq. (16). In contrast, for lower values of K'_{gs}, E will make a greater contribution, meaning

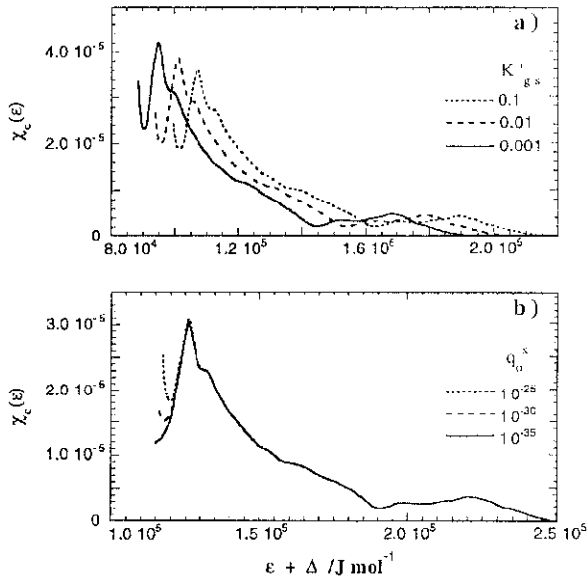

Fig. 7 Energy distribution function $\chi_c(\varepsilon)$ calculated from Eqs (26)–(32), when a) $q_0^s=10^{-20}$ Pa^{-1} for three different values of the parameter K'_{gs}; b) for different values of q_0^s and K'_{gs} with $q=q_0^s/K'_{gs}=10^{-23}$ Pa^{-1}

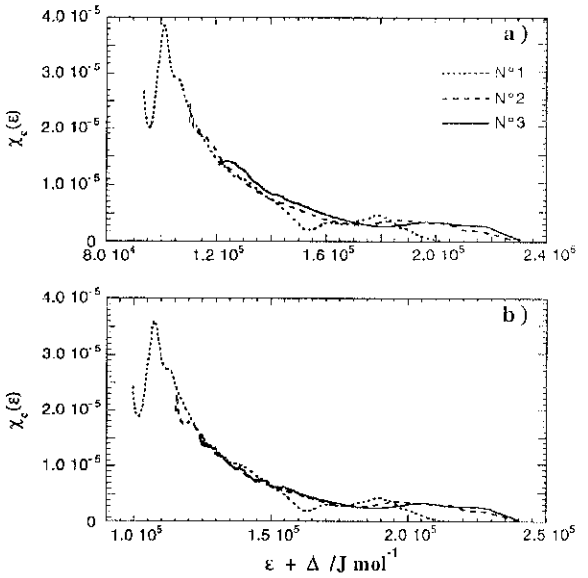

Fig. 8 Energy distribution function $\chi_c(\varepsilon)$ calculated from Eqs (26)–(32), when $q_0^s=10^{-20}$ Pa^{-1} and a) $K'_{gs}=0.01$ Pa and b) $K'_{gs}=1$ Pa

that the actual condensation energy is lower and different from the equilibrium condensation energy. This effect is illustrated in Fig. 7a for the case of experiment 3, with q_o^s and various values of K'_{gs}. A slight expansion of the energy scale is also observed when K'_{gs} decreases. K'_{gs} thus has an effect which is the reverse of that observed for q_o^s in the case of equilibrium.

As the effect of q_o^s is already known, it appears of interest to study the effects of changing the two parameters simultaneously. Figure 7b was obtained from experiment 3 by keeping constant the parameter $q=q_o^s/K'_{gs}$, defined in the previous section. This example shows that these two parameters have quantitatively equal, but opposite effects. Only small differences are observed on the low-energy side, because of the choice of $\varepsilon_c(t=0)$.

From a practical point of view, K'_{gs} should be chosen high enough to limit the related effect on the energy shift in experiment 1, which is close to equilibrium. The curves obtained for the three experiments with $q_o^s=10^{-20}$ and $K'_{gs}=1$ and 0.01 are presented in Fig. 8. As observed for the desorption kinetics only, the numerical procedure smoothes the experimental noise. Acceptable superposition is observed for higher values of K'_{gs} except for the high-energy range in experiment 3, due to experimental errors. For lower values of K'_{gs}, the energy shifts for the distributions computed from experiments 2 and 3 are too important with regard to the energy scale of the distribution deduced from experiment 1.

Discussion

On the choice of the approach used to calculate the adsorption energy distribution

In order to compare the three different approaches developed in this paper, the three condensation energy distributions $\chi_c(\varepsilon_c)$ calculated by assuming equilibrium (Eq), desorption only (Dr) and desorption-readsorption conditions (DRr) are presented in Fig. 9 for each experiment when $q=10^{-20}$. As expected, kinetic equations are to be used in order to arrive at superposition of the different curves.

For a constant heating rate, the Eq. assumption can not be used. The superimposition of the distribution obtained by using the Dr and DRr assumptions confirms the fact that the desorption rate is much more important than the readsorption rate. Distribution curves can then be computed safely from the Dr approach, as mentioned in a paper devoted to TPD [43].

For a controlled desorption rate, two situations are observed. Experiment 2 can be treated as experiment 3, using the Dr or DRr conditions, while for experiment 1, the Dr condition can not be used as this experiment is close to equilibrium.

The DRr approach appears the most useful one, therefore, as it allows an analysis of quasi-equilibrium conditions and actually non-equilibrium conditions using the same equation.

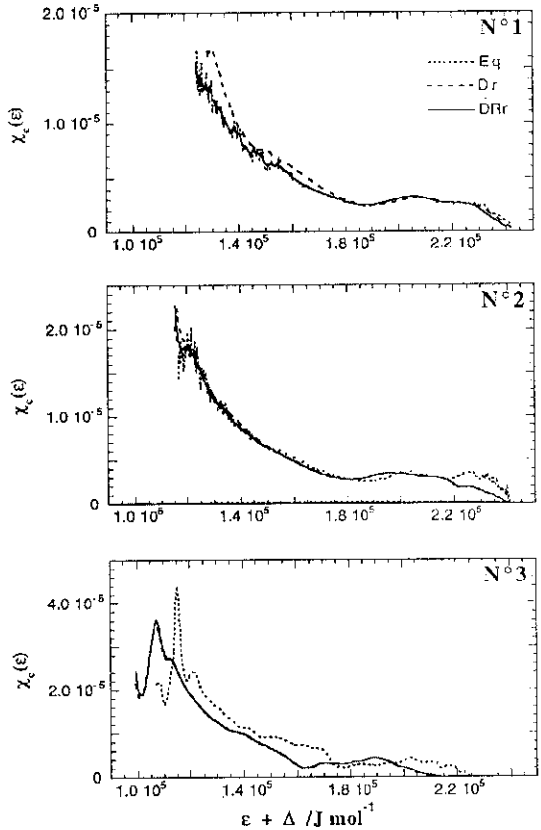

Fig. 9 Energy distribution function $\chi_c(\varepsilon)$ calculated for the equilibrium (Eq), desorption only (Dr) and desorption and readsorption (DRr) assumptions for $q=10^{-20}$ Pa^{-1}

From the experimental point of view, the constant heating rate method exhibits some other limitations, as inaccurate temperature and pressure values can be recorded, especially in the high-temperature range. In contrast, the constant desorption rate method appears to be a very promising one for studies of surface heterogeneity, as it allows the establishment of desorption isobar curves. For this latter method, one single parameter varies, while in classical TPD, the temperature and pressure vary simultaneously.

On the energy scale

Finally, the energy scale has to be discussed, as the estimated energies of adsorption appear to be higher than expected. The main problem now is to determine the unknown parameter Δ, in order to obtain the true energy scale. For instance, if the lowest energy point of experiment 3 is used as a reference, the energy scale appears correct (Fig. 10) as the low-energy part is compatible with

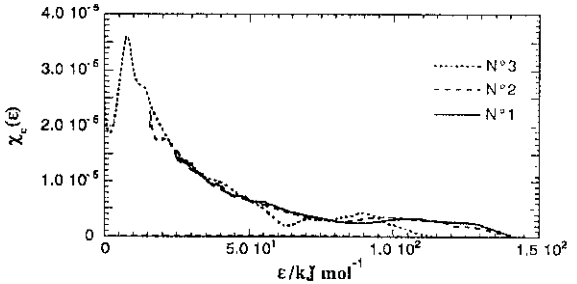

Fig. 10 Normalized energy distribution function $\chi_c(\varepsilon)$ calculated from Eqs (26)–(32), when $q_o^s=10^{-20}$ Pa^{-1} and $K'_{gs}=1$ Pa and with Δ taken as the lowest value of ε of experiment 3

physisorption (order 20 kJ mol^{-1}), while the high-energy range corresponds to chemisorption (order 100 kJ mol^{-1}). From an experimental point of view, Δ could be estimated by using in the experiments samples saturated with water, and by starting the desorption at lower temperatures. A special experimental set-up is now under construction in our laboratory, which will make it possible to perform controlled rate experiments starting at 173 K. This set-up will also provide a possibility to maintain controlled rate conditions, and to study the whole monolayer desorption range for lower pressures.

Conclusions

The controlled rate thermal analysis set-up appears to be a promising experimental technique for studies of surface heterogeneity from the desorption of preadsorbed species. It allows classical TPD analysis and also the measurement of desorption isobars. A single approach, based on the statistical rate theory of interfacial transport, allows determination of the condensation energy distribution from experiments performed in these different ways, by taking into account both the desorption and readsorption rates.

* * *

The authors, and especially W. Rudzinski, wish to express their thanks to the French Ministry of Education and Research for the grant facilitating the extended visits by W. R. to the Laboratoire Environnement et Minéralurgie.

References

1 M. Jaroniec and R. Madey (Eds.), Physical Adsorption on Heterogeneous Solids, Elsevier, Amsterdam 1988.
2 W. Rudzinski and D. H. Everett (Eds.), Adsorption of Gases on Heterogeneous Surfaces, Academic Press, London 1992.
3 Y. Amenomiya and R. J. Cvetanovic, J. Phys. Chem., 67 (1963) 144.
4 R. J. Cvetanovic and Y. Amenomiya, Adv. Catal., 17 (1967) 320.

5 R. J. Cvetanovic and Y. Amenomiya, Catal. Rev., 6 (1972) 21.
6 I. L. Falconer and I. A. Schwarz, Catal. Rev.-Sci. Eng., 25 (1983) 141.
7 I. L. Lemaitre, in F. Delannay (Ed.) Characterization of Heterogeneous Catalysts, Marcell Dekker Inc., New York 1984, Chapt. 2.
8 S. Bhatia, I. Beltramini and D. D. Do, Catal. Today, 8 (1990) 309.
9 S. J. Lombardo and A. T. Bell, Surf. Sci. Rep., 13 (1991) 1.
10 J. Rouquerol J., J. Thermal Anal., 2 (1970) 123.
11 J. Rouquerol J., J. Thermochim. Acta, 144 (1989) 209.
12 J. Rouquerol, S. Bordère and F. Rouquerol, Thermochim Acta, 203 (1992) 193.
13 L. Erdey, F. Paulik and J. Paulik, Hungarian Patent N° 152197, registered 31 October 1062, published 1 December 1965.
14 J. Paulik and F. Paulik, in Svehla (Ed.) Comprehensive Analytical Chemistry, Elsevier, Amsterdam, 1981, Vol. XII, Part A., p. 48.
15 F. Paulik and J. Paulik, Thermochim. Acta, 100 (1986) 23.
16 A. Clark (Ed.), The Theory of Adsorption and Catalysis, Academic Press, London 1970.
17 V. P. Zhdanov, Surf. Sci. Rep., 12 (1991) 183.
18 E. G. Seebauer, A. C. F. Kong and L. D. Schmidt, Surf. Sci., 193 (1988) 417.
19 P. Kisliuk, J. Phys. Chem. Solids, 3 (1957) 95.
20 D. A. King, Surf. Sci., 64 (1977) 43.
21 R. Gorte and L. D. Schmidt, Surf. Sci., 76 (1978) 559.
22 K. Nagai, Phys. Rev. Lett., 54 (1985) 2159.
23 K. Nagai, Surf. Sci., 176 (1986) 193.
24 J. H. de Boer, Adv. Catal., 8 (1956) 89.
25 K. Nagai and A. Hirashima, Surf. Sci., 171 (1986) L464.
26 A. Cassuto, Surf. Sci., 203 (1988) L656.
27 K. Nagai, Surf. Sci., 203 (1988) L659.
28 K. Nagai, Surf. Sci. Lett., 224 (1991) L147.
29 H. J. Kreuzer and S. H. Payne, Surf. Sci., 198 (1988) 235; Surf. Sci., 200 (1988) L433.
30 S. H. Payne and H. J. Kreuzer, Surf. Sci., 205 (1988) 153; Surf. Sci., 222 (1989) 404.
31 H. J. Kreuzer and S. H. Payne, in C. T. Rettner and M. N. R. Ashfold (Eds.) Dynamics of Gas-Surface Interaction, The Royal Society of Chemistry, Thomas Graham House, Science Park, Cambridge 1991, Chapt. 6.
32 H. J. Kreuzer and S. H. Payne, in W. Rudzinski et al. (Eds.) Equilibria and Dynamics of Gas Adsorption on Heterogeneous Solid Surfaces, Elsevier, Amsterdam 1977, p. 153.
33 C. A. Ward and R. D. Findlay, J. Chem. Phys., 76 (1982) 5615.
34 J. A. Eliot and C. A. Ward, in W. Rudzinski et al. (Eds.) Equilibria and Dynamics of Gas Adsorption on Heterogeneous Solid Surfaces, Elsevier, Amsterdam 1997, p. 285.
35 C. A. Ward and M. Elmoselhi, Surf. Sci., 176 (1986) 457.
36 Y. Grillet, J. M. Cases, M. François, J. Rouquerol and J. E. Poirier, Clays and Clay Minerals, 36 (1988) 233.
37 J. M. Cases, Y. Grillet, M. François, L. Michot, F. Villiéras and J. Yvon, Clays and Clay Minerals, 39 (1991) 191.
38 I. Berend, J. M. Cases, M. François, J. P. Uriot, L. J. Michot, A. Masion and F. Thomas, Clays and Clay Minerals, 43 (1995) 324.
39 J. M. Cases, I. Berend, M. François, J. P. Uriot, L. J. Michot and F. Thomas, Clays and Clay Minerals, 45 (1997) 8.
40 L. J. Michot, F. Villiéras, M. François, J. Yvon, R. Le Dred and J. M. Cases, Langmuir, 10 (1994) 3765.
41 L. J. Michot, F. Didier, F. Villiéras and J. M. Cases, Polish J. Chem., 71 (1997) 665.
42 M. J. Torralvo, Y. Grillet, F. Rouquerol and J. Rouquerol, J. Thermal Anal., 41 (1994) 1529.
43 W. Rudzinski, in W. Rudzinski et al. (Eds.) Equilibria and Dynamics of Gas Adsorption on Heterogeneous Solid Surfaces, Elsevier, Amsterdam 1997, p. 335.